

Electron-impact-excitation cross sections of lithiumlike ions

V. I. Fisher, Yu. V. Ralchenko, V. A. Bernshtam, A. Goldgirsh, and Y. Maron
Faculty of Physics, Weizmann Institute of Science, Rehovot 76100, Israel

L. A. Vainshtein
P. N. Lebedev Physical Institute, Russian Academy of Sciences, Moscow 117924, Russia

Igor Bray
Electronic Structure of Materials Centre, School of Physical Sciences, The Flinders University of South Australia, G.P.O. Box 2100, Adelaide 5001, Australia
 (Received 23 April 1997)

We present an easy to use expression for cross sections of electron-impact-induced $1s^2nl \rightarrow 1s^2n'l'$ excitation transitions with $2 \leq n \leq n' \leq 4$ in multiply charged ions of lithium isoelectronic sequence. This expression is based on our computations by convergent close-coupling (CCC) and Coulomb-Born with exchange and normalization (CBE) methods. We show scaling of the CCC and CBE cross sections with atomic number Z and use this scaling for presentation of the cross-section data. For $6 \leq Z \leq 30$ the scaling is accurate to better than $\pm 20\%$ at any energy except in the vicinity of resonances. Contributions from indirect excitation channels do not scale with Z ; however, for calculation of excitation rates it is enough to average locally these contributions over energy and to take them into account in a frame of a general scaling-based expression for the cross sections. For excitation rates, total inaccuracy caused by all simplifications in the cross-section presentation is likely to be less than $\pm 30\%$ even for most risky cases. This assessment is based on comparison of excitation rates, computed using our scaling-based expression for the cross sections, with the excitation rates, computed using high-resolution (CCC and R matrix) cross sections and experimental data. [S1050-2947(97)06211-2]

PACS number(s): 34.80.Kw

I. INTRODUCTION

Interpretation of spectroscopic measurements in plasma physics and astrophysics, as well as subsequent analysis of kinetic and transport processes in space and laboratory plasmas, are based on models of the plasma composition, i.e., on assumptions chosen for computation of ionization-stage and quantum-state abundances. For plasmas that are not in local thermodynamic equilibrium, such computations require full-energy-range cross sections of electron-impact excitation of ions. Although many cross sections are determined experimentally or computed rather accurately for some intervals of incident electron energy,¹ these data meet only a small part of the total requirement of plasma physics and astrophysics. In the case of non-Maxwellian plasmas (observed, for example, in solar flares, high-intensity radiation fields, strong shock waves, plasma lasers, z -pinches, x -pinches, tokamaks,

plasma focuses, plasma opening switches, and other pulsed-power devices) the requirement of applications is met even less because in the case of non-Maxwellian electron energy distribution one cannot use data published in the form of Maxwell-average rates and effective collision strengths.²

In this paper we suggest and discuss an easy to use and reasonably accurate expression for excitation cross sections of multiply charged lithiumlike ions (more precisely, for full-energy-range $1s^2nl \rightarrow 1s^2n'l'$ cross sections with $2 \leq n \leq n' \leq 4$ in ions with atomic number $Z \geq 6$). This paper is structured as follows: Sec. II contains brief descriptions of the convergent close-coupling (CCC) and Coulomb-Born with exchange and normalization (CBE) methods used in our computations. In Sec. III we present the cross sections computed for a few ions, show their scaling with Z , suggest a general scaling-based expression for the cross sections in a broad Z range, and discuss distortions of the scaling caused by relativistic effects and contributions from indirect excitation channels. In Sec. IV the computational cross sections and excitation rates are compared with experimental data. In Sec. V we summarize the results and discuss the general problem of cross-section data presentation for applications.

¹Brief information on excitation cross sections studied before 1995 may be found in annotated compilations by Itikawa and co-workers [1], measurements of excitation rates are discussed by Griem [2] and Kunze with co-workers [3], an evaluated compilation of theoretical data sources available through the mid-1990 is published by Pradhan and Gallagher [4], and a few overviews of data for ions of major interest are published as proceedings of the Atomic Data Assessment Meeting [5]. Most data mentioned above and more recent information may be found in atomic databases accessible via computer networks (see, for example, URL <http://plasma-gate.weizmann.ac.il/DBfAPP.html>).

²Actually, there were a few attempts to use Maxwellian rates for simulation of non-Maxwellian plasmas. They are based on assumptions of bi-Maxwellian or three-Maxwellian distributions of electrons. However, these assumptions are not due to physical arguments but because there was no option (in the codes used) to compute rates for arbitrary electron energy distribution.

II. THE CCC AND CBE METHODS

The CCC method is presented in Refs. [6–9]. The basic idea of the CCC approach to electron-atom and electron-ion collisions is to solve the coupled equations arising upon expansion of the total wave function in a truncated Laguerre basis of size N . This basis size is increased until convergence to a desired accuracy is observed. The usage of the Laguerre basis ensures that all states in the expansion are square integrable, and so gives a discretization of the target continuum as well as a good representation of the target true discrete spectrum. For a sufficiently large N , pseudoresonances, associated with the target continuum discretization, diminish substantially so that no averaging is necessary. The CCC cross sections are in excellent agreement with experimental results available for various targets (see, for example, Refs. [7,8,10,11]). However, CCC computations are very time consuming. Therefore, at present the CCC cross sections with high resolution of resonant intervals have been generated only for a fraction of the transitions required in applications. For detailed study of resonance transitions there are now two R -matrix-with-pseudostates (RMPS) approaches due to Bartschat *et al.* [12] and Badnell and Gorczyca [13], which are able to efficiently generate close-coupling results on a fine energy mesh and also take the target continuum into account.

Generally, for highly charged targets the importance of treating the target continuum is substantially diminished. This allows us to run the CCC code in the standard close-coupling mode, where only true discrete states are coupled together. The CCC cross sections presented in this paper have been obtained using $n \leq 7$ discrete states. At all given energies, away from resonances, the cross sections are estimated to be within 10% of the true nonrelativistic model solution for the considered $Z \geq 6$ scattering systems. The recent papers on Be^+ (i.e., for $Z=4$) and B^{2+} [11,14] suggest that for a few transitions in C^{3+} the effect of the target continuum may still be substantial at some intermediate energies. This invites further investigation, but does not affect the present scaling considerations.

The CBE cross sections are calculated by the ATOM computer code [15]. In this code, exchange is taken into account by the method of orthogonalized functions and the normalization is done by the K -matrix method for one channel [16]. ATOM has an option to compute the cross sections for prescribed (say, experimentally determined) transition energies, and commonly we use this option to increase accuracy. ATOM executes quickly and enables the generation of tens of cross sections per day using a personal computer.

Comparisons performed for hydrogenlike ions showed that for nonresonant energies and highly charged ions the CBE and CCC cross sections agree with each other to better than 10% [17]. Let us also note that CCC and CBE methods provide correct values of scaled collision strengths [18] in the nonrelativistic $x \rightarrow \infty$ limit.

Typically, we compute each CBE cross section for 20 energies distributed logarithmically over the $1.02 \leq x \leq 200$ interval. Here x is the ratio of the incident electron kinetic energy ε to the transition energy $\Delta E \equiv |E_{n'l'} - E_{nl}|$. The kinetic energy of the free electron ε is relative to the lower state of the transition.

TABLE I. Coefficients $a_{nl,n'l'}$, $b_{nl,n'l'}$, $\gamma_{nl,n'l'}$, $\delta_{nl,n'l'}$, and $\zeta_{nl,n'l'}$ for monopole transitions.

Transition	$a_{nl,n'l'}$	$b_{nl,n'l'}$	$\gamma_{nl,n'l'}$	$\delta_{nl,n'l'}$	$\zeta_{nl,n'l'}$
$2s-3s$	1.46	0.07	31.8	-20.8	15.5
$2s-4s$	1.95	0.23	2.63	-1.31	0.702
$2p-3p$	2.01	0.05	36.0	-31.6	33.0
$2p-4p$	2.03	0.06	4.83	-2.59	4.07
$3s-4s$	1.50	-0.00	524	-441	320
$3p-4p$	1.28	-0.17	1110	-1020	855
$3d-4d$	1.97	0.01	418	-194	268

III. THE CROSS SECTIONS AND THEIR Z SCALING

The CCC code is applied to generate the cross sections for C^{3+} , Ne^{7+} , and Al^{10+} (namely, $1s^2nl \rightarrow 1s^2n'l'$ cross sections with $n \leq 3$, $n' \leq 4$). The ATOM code is applied to generate the cross sections for C^{3+} , Ne^{7+} , Al^{10+} , and Ar^{15+} (namely, $1s^2nl \rightarrow 1s^2n'l'$ cross sections with $n \leq n' \leq 4$ except for $4d-4f$). The $4d-4f$ cross section is excluded because ATOM does not provide sufficient accuracy in the case of small transition energy, namely, for $\Delta E < 0.1$ eV. Here, we shall denote each $1s^2nl \rightarrow 1s^2n'l'$ cross section by $\sigma_{Z,nl,n'l'}(x)$.

A. Scaling law

Analysis of the cross sections shows that for any pair of initial ($1s^2nl$) and final ($1s^2n'l'$) states there are two constants (say, $a_{nl,n'l'}$ and $b_{nl,n'l'}$) that enable one to transform rather accurately Z -dependent cross sections $\sigma_{Z,nl,n'l'}(x)$ into Z -independent (scaled) cross sections $s_{nl,n'l'}(x)$. This scaling law may be presented by the expression

$$(Z - a_{nl,n'l'})^{(4 - b_{nl,n'l'})} \sigma_{Z,nl,n'l'}(x) / \pi a_0^2 = s_{nl,n'l'}(x). \quad (1)$$

Here a_0 is the Bohr radius. The constants $a_{nl,n'l'}$ and $b_{nl,n'l'}$ computed using the CCC and CBE cross sections are presented in Tables I–IV for monopole ($l'=l$), dipole ($l'=l \pm 1$), quadrupole ($l'=l \pm 2$), and octupole ($l'=l \pm 3$) transitions, respectively.

We treat the $a_{nl,n'l'}$ and $b_{nl,n'l'}$ as scaling parameters only. However, for most of the transitions $a_{nl,n'l'}$ has values from 0 to 2, like the screening constant. The $b_{nl,n'l'}$ values are small ($b_{nl,n'l'} \leq 4$) but nonzero, in contrast to true one-electron ions (see, for example, Ref. [17]).

B. Presentation of the cross sections by analytical function

To present the CCC and CBE cross sections $\sigma_{Z,nl,n'l'}(x)$ in an easy to use form, we fitted them by a function

$$\sigma_{Z,nl,n'l'}^f(x) = \pi a_0^2 (Z - a_{nl,n'l'})^{-(4 - b_{nl,n'l'})} s_{nl,n'l'}^f(x), \quad (2)$$

which takes into account the scaling (1) and assumes a reasonable dependence on electron energy, namely,

TABLE II. Coefficients $a_{nl,n'l'}$, $b_{nl,n'l'}$, $\eta_{nl,n'l'}$, $\gamma_{nl,n'l'}$, $\delta_{nl,n'l'}$, and $\zeta_{nl,n'l'}$ for dipole transitions.

Transition	$a_{nl,n'l'}$	$b_{nl,n'l'}$	$\eta_{nl,n'l'}$	$\gamma_{nl,n'l'}$	$\delta_{nl,n'l'}$	$\zeta_{nl,n'l'}$
2s-2p	-0.04	0.47	1764	2268	3569	-1190
2s-3p	-0.77	-0.42	449.4	-476.9	838.5	-219.9
2s-4p	0.60	0.01	13.37	-6.49	8.68	5.11
2p-3s	2.54	-0.20	5.53	-4.009	7.705	0.8263
2p-4s	2.64	0.01	0.5353	-0.4272	0.8667	0.4139
2p-3d	1.07	-0.20	300.8	40.22	28.40	220.1
2p-4d	2.01	0.09	10.36	8.004	-4.986	11.35
3s-3p	0.25	0.61	32720	-16 820	188 600	-102 100
3s-4p	-0.75	-0.46	4128	-5213	9356	-3163
3p-4s	2.61	-0.25	109.4	-119.2	221.9	-57.01
3p-3d	1.56	0.50	34880	-11 820	219 200	-138 000
3p-4d	1.68	0.05	888.2	-667	1477	-349.6
3d-4p	1.76	-0.33	60.07	-38	264.7	-51.03
3d-4f	1.27	-0.20	4279	-2650	8056	-1777
4s-4p	-0.72	0.01	1 514 000	-859 300	6 751 000	-3 091 000
4p-4d	0.57	0.01	2 105 000	-2 200 000	6 615 000	1 802 000

$$s_{nl,n'l'}^f(x) = x^{-1}(\eta_{nl,n'l'} \ln x + \gamma_{nl,n'l'} + \delta_{nl,n'l'} x^{-1} + \zeta_{nl,n'l'} x^{-2}). \quad (3)$$

Values of $\eta_{nl,n'l'}$, $\gamma_{nl,n'l'}$, $\delta_{nl,n'l'}$, and $\zeta_{nl,n'l'}$ are listed in Tables I–IV. The function $s_{nl,n'l'}^f(x)$ may be interpreted as analytical presentation of computational results scaled by the factor $\pi a_0^2 (Z - a_{nl,n'l'})^{-(4-b_{nl,n'l'})}$.

The coefficients $\eta_{nl,n'l'}$, $\gamma_{nl,n'l'}$, $\delta_{nl,n'l'}$, and $\zeta_{nl,n'l'}$ provide accurate fits of nonrelativistic cross sections in the $x \rightarrow \infty$ limit as well. Transformation of nonrelativistic high-energy asymptotics of any cross section into a relativistic one may be done by attaching a relativistic tail (see, for example, Ref. [19] and references therein) to a nonrelativistic cross section (2) at some reasonably large value of x .

Practically for any energy, except relatively narrow intervals around some of the resonances, the function $\sigma_{Z,nl,n'l'}^f(x)$ fits CCC and CBE cross sections to better than $\pm 20\%$. So far, we have computed CCC and CBE cross sections for $Z \leq 18$ only; however, one can see below that the function $\sigma_{Z,nl,n'l'}^f(x)$ provides sufficient accuracy for much larger values of Z as well.

TABLE III. Coefficients $a_{nl,n'l'}$, $b_{nl,n'l'}$, $\gamma_{nl,n'l'}$, $\delta_{nl,n'l'}$, and $\zeta_{nl,n'l'}$ for quadrupole transitions.

Transition	$a_{nl,n'l'}$	$b_{nl,n'l'}$	$\gamma_{nl,n'l'}$	$\delta_{nl,n'l'}$	$\zeta_{nl,n'l'}$
2s-3d	1.11	0.01	118	-162	106
2s-4d	1.52	0.01	12	-13.7	9.9
2p-4f	2.09	0.10	5.45	-8.65	7.33
3s-3d	2.07	1.01	810	90.5	10.5
3s-4d	1.21	0.14	620	-851	509
3p-4f	1.83	0.02	1010	-1300	942
3d-4s	2.86	0.01	9.43	-8.42	11.8
4s-4d	-0.87	0.01	316 000	33 700	-39 400
4p-4f	0.73	0.01	200 000	45 600	-10 100

C. High-Z limit of the scaling

To find the high-Z limit of the scaling law (1) we scaled relativistic distorted wave (RDW) cross sections available³ for atomic numbers from 8 to 92 [20]. Scaled RDW cross sections

$$(Z - a_{nl,n'l'})^{(4-b_{nl,n'l'})} \sigma_{Z,nl,n'l'}^{\text{RDW}}(x) / \pi a_0^2$$

are compared with the function $s_{nl,n'l'}^f(x)$, which presents scaled CCC and CBE cross sections for $6 \leq Z \leq 18$.

In Fig. 1 one can see such comparison for 2s-4p transitions in ions with $6 \leq Z \leq 92$. For $x > 1.5$ scaled RDW cross sections of all ions with $Z \leq 57$ go within a $\pm 20\%$ range around the function $s_{2s,4p}^f(x)$. Even for U^{89+} the deviation from the scaling is by less than a factor of 2. Deviations of scaled CBE and RDW cross sections from $s_{2s,4p}^f(x)$ in the near-threshold energy domain ($1 < x < 1.5$) are caused by the inaccuracy of CBE and RDW methods, which ignore contributions from indirect excitation channels. The CCC method takes these contributions into account; therefore, the function $s_{nl,n'l'}^f(x)$ is designed in such a way that at $x \approx 1$ it follows mainly the CCC cross sections. More details on the resonances are given in Sec. II E.

For each transition one can find some atomic number $Z_{nl,n'l'}$ that separates the small-Z range, where relativistic effects are small (for nonrelativistic energies), from the high-Z range, where relativistic effects cause substantial distortion of the scaling at any energy. In the case of the 2s-4p transition, considered above, scaled RDW cross sections of ions with $Z \leq 57$ go within a $\pm 20\%$ range around the function $s_{nl,n'l'}^f(x)$; therefore, we may say that $Z_{2s,4p} = 57$ is the upper limit of the scaling for which relativistic distortion equals 20%. For all 2p- $n'l'$ and 2s- $n'l'$ transitions, except 2s-2p, the comparisons with RDW cross sections

³Excitation from the 2s and 2p states.

TABLE IV. Coefficients $a_{nl,n'l'}$, $b_{nl,n'l'}$, $\gamma_{nl,n'l'}$, $\delta_{nl,n'l'}$, and $\zeta_{nl,n'l'}$ for octupole transitions.

Transition	$a_{nl,n'l'}$	$b_{nl,n'l'}$	$\gamma_{nl,n'l'}$	$\delta_{nl,n'l'}$	$\zeta_{nl,n'l'}$
$2s-4f$	1.15	0.01	4.55	-3.91	4.53
$3s-4f$	1.53	0.01	431	-225	215
$4s-4f$	3.17	1.25	391	110	-85.1

show $Z_{2l,n'l'} > 50$. For the $2s \rightarrow 2p$ transition the comparison shows a much lower limit, namely, $Z_{2s,2p} = 30$. This difference in $Z_{nl,n'l'}$ limits is caused by a substantial difference in threshold energies for $2s \rightarrow 2p_{1/2}$ and $2s \rightarrow 2p_{3/2}$ transitions. The ratio

$$\Gamma_{2s,2p} = \frac{|E_{2p_{3/2}} - E_{2p_{1/2}}|}{|E_{2p} - E_{2s}|}$$

is much larger than any other ratio

$$\Gamma_{nl,n'l'} = \frac{|E_{n'l',l'+1/2} - E_{n'l',l'-1/2}|}{|E_{nl} - E_{n'l'}|},$$

introduced for $nlj \rightarrow n'l'j'$ transitions with the same Z (however, note that at present relativistic cross sections are available for transitions from $2s$ and $2p$ states [20]) only. The $\Gamma_{2s,2p}$ ratio increases drastically with Z (for example, $\Gamma_{2s,2p} = 0.58\%$, 9.3% , 38% , and 68% for $Z=8$, 18 , 30 , and 40 , respectively); therefore, the x scales for $2s \rightarrow 2p_{1/2}$ and $2s \rightarrow 2p_{3/2}$ cross sections are different. This difference in scales distorts a scaling over $\varepsilon/|E_{2p} - E_{2s}|$. In general, for all transitions with $n'=n$, the $\Gamma_{nl,n'l'}$ ratios are much larger than for transitions with $n' \neq n$; therefore, we expect to have lower $Z_{nl,n'l'}$ limits for all transitions with $n'=n$.

D. Low- Z limit of the scaling

The scaling law (1) is found for *multiply* charged ions. For Ne^{7+} and Al^{10+} the CCC and CBE cross sections deviate from the functions $\sigma_{Z,nl,n'l'}^f(x)$ by much less than 20% (for

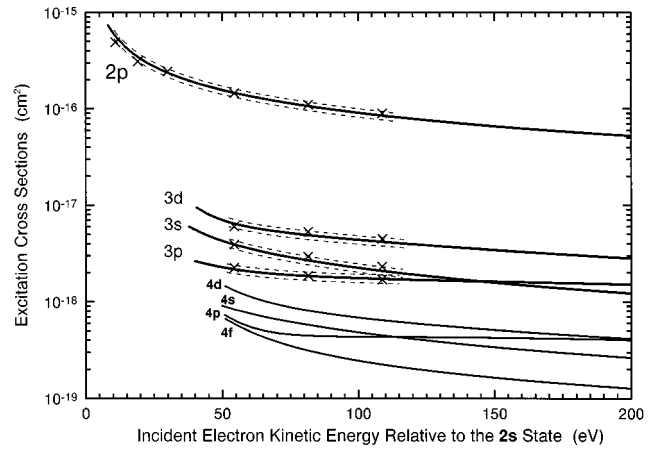


FIG. 2. Excitation cross section of $2s-n'l'$ transitions in C^{3+} . Full curves present cross sections given by expression (2). Dashed curves present $\pm 10\%$ error bars around them. Crosses present nine-state CC computations tabulated in Ref. [22].

nonresonant energies). For *triply* charged C^{3+} scaled CCC and CBE cross sections deviate from $\sigma_{nl,n'l'}^f(x)$ noticeably, but still by less than 20%. On the basis of these observations for low- Z ions and taking into account the $Z \leq 30$ restriction derived in Sec. III C, we believe that cross sections (2) provide an accuracy to better than $\pm 20\%$ for atomic numbers belonging to the interval

$$6 \leq Z \leq 30. \quad (4)$$

Nine-state close-coupling R -matrix (RM) cross sections available for a few transitions in C^{3+} [22] also agree with the scaling to better than $\pm 20\%$. One can see this in Fig. 2 where solid curves present functions $\sigma_{6,2s,n'l'}^f(x)$, dashed curves mark $\pm 10\%$ ranges around them, and crosses present tabulated RM data from Ref. [22]. These data deviate from $\sigma_{6,2s,n'l'}^f(x)$ by less than 15%.

Besides the accuracy of presentation of the cross sections by the functions $\sigma_{Z,nl,n'l'}^f(x)$, Fig. 2 exhibits relations of the

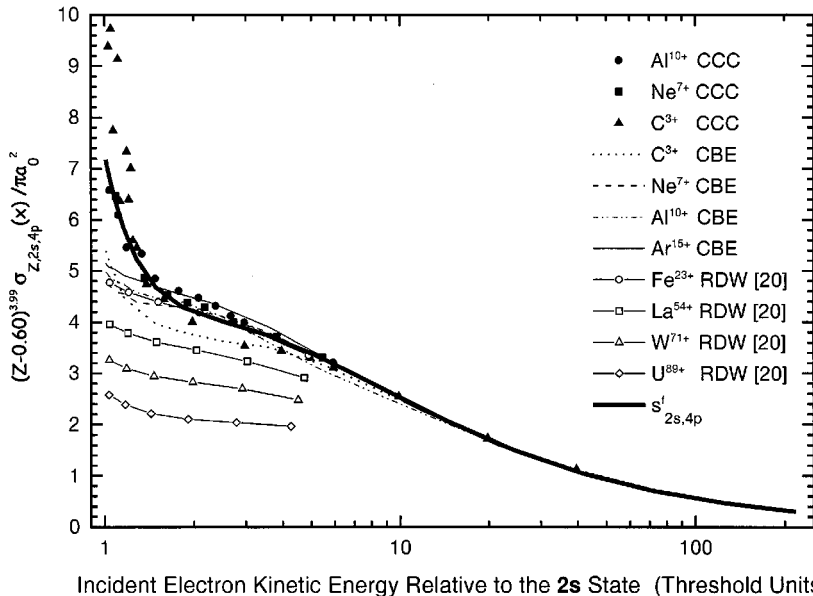


FIG. 1. Scaled $2s-4p$ excitation cross sections of ions with atomic numbers from 6 to 92.

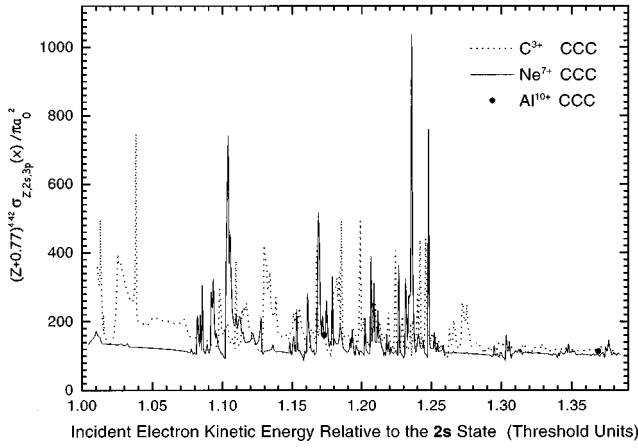
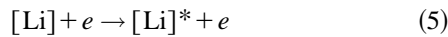


FIG. 3. Scaled CCC cross sections for $2s-3p$ excitation of C^{3+} , Ne^{7+} , and Al^{10+} in the region of resonances.

cross sections with different Δn and Δl . The cross section with $\Delta n=0$ is about a factor of 20 larger than the cross sections with $\Delta n=1$ and about a factor of 100 larger than the cross sections with $\Delta n=2$. In each set of the cross sections with certain Δn quadrupole cross sections dominate over monopole and octupole cross sections. However, monopole transitions have a significant advantage over other non-dipole transitions in cross section per unit level, i.e., in the $\sigma_{Z,nl,n'l'}(x)/g_{n'l'}$ ratio. Here $g_{n'l'}$ is the degeneracy of the $n'l'$ state. Dipole cross sections are substantially smaller than quadrupole and monopole ones (with the same Δn) in the near-threshold energy domain but at $x \gg 10$ dipole cross sections are larger than all nondipole cross sections because of the weaker asymptotic dependence on x (namely, $x^{-1} \ln x$ vs x^{-1}).

E. Contributions from indirect channels

The CBE and RDW approximations take into account direct (one-step) excitation

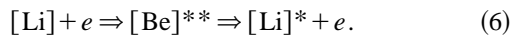


only and generate smooth cross sections $\sigma_{Z,nl,n'l'}(x)$, which scale rather accurately with Z . Scaled cross sections

$$(Z - a_{nl,n'l'})^{(4 - b_{nl,n'l'})} \sigma_{Z,nl,n'l'}^{\text{CBE,RDW}}(x) / \pi a_0^2$$

may be fitted by smooth Z -independent functions $s_{nl,n'l'}^f(x)$, which provide acceptable accuracy of the presentation (2) at any energy and for a broad range of atomic numbers.

The close coupling (CC) approximation takes into account direct excitation (5) and two-step excitation via doubly excited states of beriliumlike ions



In Fig. 3 we present scaled CCC cross sections for $Z=6, 10$, and 13 . One can see that contributions from indirect channels do not scale with Z and distort scaling of the cross sections in general. Moreover, these contributions form irregular sequences of resonant spikes that cannot be presented accu-

rately by easy-to-use expressions or by short electronic files acceptable for further use in applications.⁴

Fortunately, plasma physicists and astrophysicists are not interested in high energy resolution of collisional cross sections. On the contrary, they operate with integrals over the entire energy range, namely, with the excitation rate coefficients

$$R_{Z,nl,n'l'}(\bar{\varepsilon}, p_e) = \int_0^\infty \sigma_{Z,nl,n'l'}(\varepsilon) v_e(\varepsilon) f_e(\varepsilon, \bar{\varepsilon}, p_e) d\varepsilon. \quad (7)$$

In this expression, $v_e(\varepsilon)$ is the electron velocity, $f_e(\varepsilon, \bar{\varepsilon}, p_e)$ is the electron energy distribution normalized to unity, $\bar{\varepsilon}$ is the mean electron energy,⁵ and p_e denotes other parameters of the distribution. Commonly, the product $v_e(\varepsilon) f_e(\varepsilon, \bar{\varepsilon}, p_e)$ changes negligibly over the width of a few resonances. Then, for integration with this product, it is sufficient to present highly resolved CCC or RMPS cross sections $\sigma_{Z,nl,n'l'}(\varepsilon)$ by easy to use smooth functions obtained by local averaging of these cross sections on a reasonable energy grid. This simplification is correct and accurate if CCC or RMPS computations provided many points for each cell of the grid. Unfortunately, for resonant energy intervals of many cross sections we have rather few CCC points: in some cases a total of about 20 random points for C^{3+} , Ne^{7+} , and Al^{10+} together. Therefore, we critically assess representativity of these random points before averaging over them. Smooth functions $s_{nl,n'l'}^f(x)$ obtained by averaging over such sparse sets of critically evaluated points are less accurate than results of correct local averaging over highly resolved CCC cross sections. However, even in this case the functions $s_{nl,n'l'}^f(x)$ provide better accuracy than functions achieved by disregarding of indirect excitation.

To assess inaccuracies caused by successive simplifications in the computational procedure and presentation of the cross sections, we compare excitation rate coefficients (7) computed using three presentations of one particular cross section, namely, (i) high-resolution CCC file, (ii) scaling-based expression (2), and (iii) underlying curve of the CCC cross section. For this assessment, we have chosen the Maxwellian distribution as the most popular one, and the $2s-3p$ transition in C^{3+} as the one promising large inaccuracy.⁶ We restrict our consideration to $T_e > 3$ eV because at lower temperature the abundance of C^{3+} in plasmas and the $2s-3p$ excitation rate are usually both negligible. The rate coefficients computed for $T_e = 3$ eV show a 29% difference for (ii)

⁴More examples of the cross sections computed with indirect channels taken into account may be found in Refs. [22–24].

⁵In the case of the Maxwellian distribution, $\bar{\varepsilon} = 3kT_e/2$.

⁶The expectation of a large inaccuracy in the $2s-3p$ excitation rate of C^{3+} is caused by three things: relatively poor scaling at $Z=6$, which is the lower limit of Z range, substantial contributions from indirect channels for small Z , and broad resonances just at the threshold of this transition, i.e., in the energy range commonly most important for excitation rates. Let us note for clarity that the CCC file for this cross section contains 600 points over energy. 576 of them are in a $1 < x < 1.4$ interval.

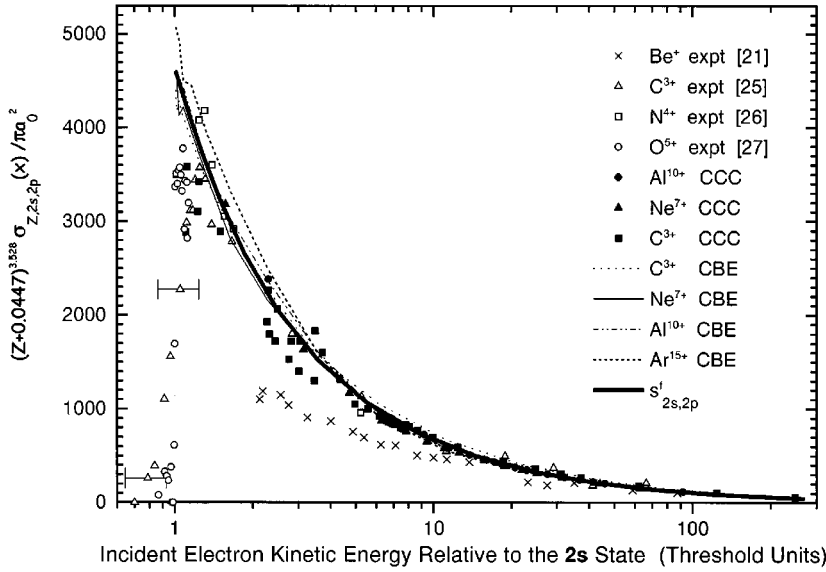


FIG. 4. Scaled $2s$ - $2p$ excitation cross sections. Full curve presents function (3). One can see that scaling law (1) is accurate to better than 20% for all *multiply* charged ions studied. The cross section of *singly* charged ion Be^+ deviates from the scaling. For better understanding of the behavior of experimental cross sections in the near-threshold energy range we show by error bars a full width at half maximum (FWHM) of the energy distribution in an electron beam; see details in the text.

versus (i) and a 41% difference for (iii) vs (i). For higher temperatures these differences [actually, inaccuracies of presentations (ii) and (iii) in comparison with the most complete presentation (i)] are less due to larger contributions to the integrals from high- x part of the cross section, which is practically one and the same in all presentations. Integrals computed for $T_e = 6$ eV show 26% inaccuracy for (ii) vs (i) and 36% for (iii) vs (i). For $T_e = 20$ eV these inaccuracies decrease to 9% and 20%, respectively. For this transition in Al^{10+} , the inaccuracies are much less at any temperature.

This comparison and estimates based on the R -matrix results for C^{3+} [22] show that excitation rates computed using expression (2) are accurate to better than $\pm 30\%$ for *any* transition in C^{3+} . For heavier ions (i.e., for $Z > 6$), an accuracy of excitation rates computed using expression (2) increases with Z because the relative contribution from two-step transitions decreases. The (iii) vs (i) comparisons show that ignoring resonances may result in larger inaccuracy than use of a scaling-based presentation of the cross sections.

IV. COMPARISON WITH EXPERIMENTAL DATA

For the excitation of lithiumlike ions, experimental results are available only for $2s$ - $2p$ cross sections, for Be^+ [21], C^{3+} [25], N^{4+} [26], and O^{5+} [27]. In Fig. 4, we compare scaled experimental cross sections with the Z -independent cross section $s_{2s,2p}^f(x)$ and scaled CCC and CBE results for this transition in C^{3+} , Ne^{7+} , Al^{10+} , and Ar^{15+} . One can see that the scaling factor

$$(Z + 0.0447)^{4 - 0.4715}$$

accommodates 10 sets of experimental and computational cross sections in a narrow ($\pm 20\%$) range around the function $s_{2s,2p}^f(x)$. These 10 sets belong to ions charged triply and more. The cross section of singly charged Be^+ (i.e., $Z = 4$) deviates from $s_{2s,2p}^f(x)$ substantially; however, we already bounded the applicability range of scaling-based cross sections (2) by $6 \leq Z \leq 30$.

Electron beams used in experiments are not monoenergetic. Therefore, each experimental point in the cross section

curve is related to the mean electron energy in the beam and presents a convolution of true excitation cross sections with the electron energy distribution in the beam [26]. Because of this convolution, each experimental curve, firstly, has its maximum not at $x = 1$ but above the threshold and, secondly, goes noticeably above zero in some below-threshold interval. For clarity, we show a FWHM of the beam (2.9 eV) for some of experimental points. This FWHM relates to both N^{4+} and C^{3+} [26].

Widths of electron beams in the experiments were too large for resolving resonant spikes [21,25–27]. Therefore, these experiments showed spike-averaged cross sections. On the other hand, it is known that contributions from indirect channels to $2s$ - $2p$ cross sections are small [28,23,24,22]. In Ref. [24] average indirect-channel-caused enhancement of $2s$ - $2p$ cross sections of C^{3+} , O^{5+} , Ne^{7+} , and Ar^{15+} was assessed as 4% only. The weakness of the effect is explained by much stronger coupling of $2s$ and $2p$ states with each other than with other states [24].

References [2,3] present excitation rate coefficients determined experimentally at some electron temperatures. 41 of these rate coefficients relate to ions with atomic numbers $6 \leq Z \leq 30$. We compared them with excitation rate coefficients computed using expression (2). The comparison showed that the rates computed agree with experimental ones to within the error bars given for experimental points.

V. SUMMARY AND CONCLUSIONS

We used CCC and CBE methods to generate cross sections of electron-impact-induced $1s^2nl \rightarrow 1s^2n'l'$ excitation transitions with $2 \leq n \leq n' \leq 4$ in C^{3+} , Ne^{7+} , Al^{10+} , and Ar^{15+} . Most of these cross sections were not published earlier.

Analysis of these and other computational and experimental cross sections showed scaling of the cross sections with atomic number Z . This scaling is expressed by relation (1).

Due to the scaling, the cross sections of lithiumlike ions may be presented by the easy to use expression (2). For ions with atomic numbers $6 \leq Z \leq 30$ the cross sections given by

expression (2) are accurate to better than 20% for any energy except in the vicinity of resonances. For each Z , in the temperature range corresponding to noticeable abundance of lithium-like ions, the Maxwellian excitation rates computed using cross sections (2) are within $\pm 30\%$ of the rates computed using highly resolved CCC or R -matrix cross sections. In general, for the $6 \leq Z \leq 30$ range, an accuracy of the excitation rates computed using expression (2) increases with Z for each transition because of decrease of relative contributions from indirect channels.

To obtain rate coefficients accurate to better than $\pm 30\%$ for any transition and any Z , one has to abandon the scaling based presentation of the cross sections and compute each cross section for atomic number of interest. Moreover, for such accuracy, the computations have to be done by a method that takes into account contributions from indirect excitation channels. Disregarding by these contributions may result in rate coefficients less accurate than scaling based ones. An example of this kind (namely, $2s-3p$ excitation rates of C^{3+} computed using highly resolved CCC cross section and an underlying curve of this cross section) was considered in Sec. III E.

At present, there are very few transitions in very few ions for which the cross sections are known with high accuracy (due to many-state CC methods). For most applications, these transitions cover only a small part of the total requirement and can improve neither the accuracy of plasma composition computations nor the reliability of interpretation of spectroscopic measurements. Therefore, less accurate (for example, scaling-based) expressions for the cross sections are helpful as well, especially if they are presented for complete sets of transitions (say, for all transitions with $n, n' < 7$), easy to use, and cover entire range of energy.

Probably, in the future many ions will be provided by

reliable cross section due to research projects analogous to the IRON Project [29]. However, computation of the cross sections and use of these cross sections in applications are always separated from each other by the procedure of data presentation. On one hand, presentation of cross sections has to provide high accuracy in rate coefficients. On the other hand, the presentation has to be convenient for plasma simulation codes. Presentation of cross section data by Maxwellian rate coefficients is suitable only for Maxwellian plasmas. For applications which deal with non-Maxwellian plasmas, such presentation is useless. A presentation of accurate, highly resolved cross sections by electronic files is reliable but it slows down plasma simulation codes drastically (because dependence of the electron energy distribution on time necessitates computing of the rates for each time step). Therefore, if the cross sections are computed for further use in applications, we recommend to present them not by files or plots but by full-energy-range fitting functions. Surely, these functions present locally averaged cross sections but this averaging reduces an accuracy of excitation rates insufficiently.

ACKNOWLEDGMENTS

We are grateful to H. R. Griem for discussions and to A. K. Bhatia, C. P. Bhalla, and S. R. Grabbe for an electronic file of cross section computed by the CC R -matrix method. This work was supported by Israel Academy of Sciences and Ministry of Sciences and Arts. The research of L.A.V. was supported by Moscow International Science and Technology Center (Grant No. 076-95) and Russian Basic Research Fond (Grant No. 97-02-16919). The research of I.B. was sponsored in part by the Phillips Laboratory, Air Force Materiel Command, USAF, under Cooperative Agreement No. F29601-93-2-0001.

-
- [1] Y. Itikawa *et al.*, *At. Data Nucl. Data Tables* **63**, 315 (1996); **49**, 209 (1991); **33**, 149 (1985); **31**, 215 (1984).
 - [2] H. R. Griem, *J. Quant. Spectrosc. Radiat. Transf.* **40**, 403 (1988).
 - [3] R. König, K.-H. Kolk, and H.-J. Kunze, *Phys. Scr.* **48**, 9 (1993).
 - [4] A. K. Pradhan and J. W. Gallagher, *At. Data Nucl. Data Tables* **52**, 227 (1992).
 - [5] *Electron Excitation Data: Reviews and Recommendations*, edited by J. Lang, *At. Data Nucl. Data Tables* **57**, 1 (1994).
 - [6] I. Bray and A. T. Stelbovics, *Phys. Rev. A* **46**, 6995 (1995).
 - [7] I. Bray, *Phys. Rev. A* **49**, 1066 (1994).
 - [8] I. Bray and A. T. Stelbovics, in *Advances in Atomic, Molecular, and Optical Physics*, edited by B. Bederson and H. Walther (Academic Press, San Diego, 1995), Vol 35.
 - [9] *Computational Atomic Physics*, edited by Klaus Bartschat (Springer-Verlag, Berlin, 1996).
 - [10] I. Bray, I. E. McCarthy, J. Wigley, and A. T. Stelbovics, *J. Phys. B* **26**, L831 (1993); **29**, L245 (1996).
 - [11] K. Bartschat and I. Bray, *J. Phys. B* **30**, L109 (1997).
 - [12] K. Bartschat, E. T. Hudson, M. P. Scott, P. G. Burke, and V. M. Burke, *J. Phys. B* **29**, 115 (1996).
 - [13] N. R. Badnell and T. W. Gorczyca, *J. Phys. B* **30**, 2011 (1997).
 - [14] P. Marchalant, K. Bartschat, and I. Bray, *J. Phys. B* **30**, L435 (1997).
 - [15] V. P. Shevelko and L. A. Vainshtein, *Atomic Physics for Hot Plasmas* (IPP, Bristol, 1993).
 - [16] I. I. Sobelman, L. A. Vainshtein, and E. A. Yukov, *Excitation of Atoms and Broadening of Spectral Lines* (Springer, Berlin, 1995).
 - [17] V. I. Fisher, Yu. V. Ralchenko, V. A. Bernshtam, A. Goldgirsh, Y. Maron, L. A. Vainshtein, I. Bray, and H. Golten, *Phys. Rev. A* **55**, 329 (1997).
 - [18] A. Burgess and J. A. Tully, *Astron. Astrophys.* **254**, 436 (1992).
 - [19] R. Jayakumar and H. H. Fleischmann, *J. Quant. Spectrosc. Radiat. Transf.* **33**, 177 (1985).
 - [20] H. L. Zhang, D. H. Sampson, and C. J. Fontes, *At. Data Nucl. Data Tables* **44**, 31 (1990).
 - [21] P. O. Taylor, R. A. Phaneuf, and G. H. Dunn, *Phys. Rev. A* **22**, 435 (1980).
 - [22] V. M. Burke, *J. Phys. B* **25**, 4917 (1992).
 - [23] J. Callaway, J. N. Gau, R. J. W. Henry, D. H. Oza, Vo Ky Lan, and M. LeDourneuf, *Phys. Rev. A* **16**, 2288 (1977).

- [24] K. Bhadra and R. J. W. Henry, *Phys. Rev. A* **26**, 1848 (1982).
- [25] P. O. Taylor, D. Gregory, G. H. Dunn, R. A. Phaneuf, and D. H. Crandall, *Phys. Rev. Lett.* **39**, 1256 (1977).
- [26] D. Gregory, G. H. Dunn, R. A. Phaneuf, and D. H. Crandall, *Phys. Rev. A* **20**, 410 (1979).
- [27] E. W. Bell, X. Q. Guo, J. L. Forand, K. Rinn, D. R. Swenson, J. S. Thompson, G. H. Dunn, M. E. Bannister, D. C. Gregory, R. A. Phaneuf, A. C. H. Smith, A. Müller, C. A. Timmer, E. K. Wählin, B. D. DePaola, and D. S. Belić, *Phys. Rev. A* **49**, 4585 (1994).
- [28] J. N. Gau and R. J. W. Henry, *Phys. Rev. A* **16**, 986 (1977).
- [29] K. A. Berrington, in *The Opacity Project* (Institute of Physics Publishing, Bristol, 1997), Vol. 2.